Observation of non-exponential relaxation above T_N in the dilute Heisenberg antiferromagnet $KMn_{0.3}Ni_{0.7}F_3$

1989 J. Phys.: Condens. Matter 1 5013

(http://iopscience.iop.org/0953-8984/1/30/016)

J. Phys.: Condens. Matter 1 (1989) 5013–5019. Printed in the UK

LETTER TO THE EDITOR

Observation of non-exponential relaxation above T_N in the dilute Heisenberg antiferromagnet $KMn_{0.3}Ni_{0.7}F_3$

R G Lloyd† and P W Mitchell‡

† Institut Laue-Langevin, BP 156X, 38042 Grenoble-Cédex, France

‡ Department of Physics, University of Manchester, Manchester M13 9PL, UK

Received 31 May 1989

Abstract. We investigate the dynamics above T_N (210 K) of the dilute Heisenberg antiferromagnet $KMn_{0.3}Ni_{0.7}F_3$ using neutron inelastic scattering. We find evidence for a long-time tail in the relaxation function at all temperatures above T_N with relaxation being much slower at and below the so-called Griffiths temperature T_G (246 K) which is the ordering temperature of pure $KNiF_3$. This is as predicted by recent theoretical studies.

Recently theoretical studies of dilute magnetic systems investigating plausible mechanisms for relaxation have predicted non-exponential forms for the long-time dynamics above the ordering temperature.

One approach [1–4] to this problem has concentrated on the dominance of the long-time dynamics of clusters of spins which are below their ordering temperature and makes a distinction between two kinds of behaviour depending on whether the system is above or below its so-called Griffiths temperature T_G, which is the ordering temperature of the corresponding pure system. This corresponds to the presence or absence of Griffiths singularities in the free energy as a function of applied magnetic field H, at $H = 0$ [5]. Non-exponential decay in the spin–spin correlation function $C(t) = [\langle S_i(t)S_i(0)\rangle]$ then emerges as the dynamical signature of the 'Griffiths phase'. This arises because of non-trivial contributions to the correlation function from large, statistically rare, quasi-ordered regions of the system whose relaxation is only limited by finite-size effects. Calculations have been performed both for Ising ($m = 1$) and vector ($m > 1$) systems. These phenomena have been investigated in computational simulations [6, 7] and a preliminary experimental study has been performed [8]. However, the results of these are inconclusive and they fail to distinguish between the 'Griffiths' phase and the paramagnetic phase. The long-time tails are analogous to those found in the problem of the density of states of an electron in a random potential [9] and the problem of a random walk with traps at random positions [10].

For Heisenberg ($m = 3$) systems below T_G the theory predicts the asymptotic $t \to \infty$ form for $C(t)$ to be

$$C(t) \sim \exp[-(Bt)^{1/2}] \tag{1}$$

the parameter B being found to vanish as $T \to T_C$ as

$$B \sim (T - T_C)^{\alpha_r + z_r \nu_r} \tag{2}$$

where α_r, ν_r and z_r are the usual critical exponents for the random system.

0953-8984/89/305013 + 07 $02.50

At and above T_G the asymptotic form is

$$C(t) \sim \exp[-t^{d/(d+z_p)} g(t/\xi_p^{d+z_p})] \tag{3}$$

with $g(x)$ a scaling function. For $t/\xi_p^{d+z_p} \gg 1$, i.e. above T_G and out of the critical region for the pure system, this is

$$C(t) \sim \exp(-c\xi_p^d) \exp(-t/\xi_p^{z_p}). \tag{4}$$

In the opposite limit, i.e. $t/\xi_p^{d+z_p} \ll 1$, which, in particular, is true in the vicinity of T_G, the prediction is

$$C(t) \sim \exp(-t^{d/d+z_p})$$

which is

$$C(t) \sim \exp(-t^{2/3}) \tag{5}$$

for $d = 3$ and $z_p = \frac{3}{2}$.

There are two main questions which the theory does not address. The first is the time regime for which the theory is expected to hold (it is not correct for short times) and thus the size of the correlation function in the region of applicability of the theory. Secondly the effect of the details of the dynamics on the applicability of the theory to real magnetic systems is not clear, model A [11] relaxational dynamics with no conservation laws being assumed in Bray's work [4] (at least below T_G).

For these reasons it is of interest to try to measure directly the relaxational dynamics to see whether these tails are visible experimentally in a real magnetic system. We have used neutron inelastic scattering as a probe of the power spectrum of the spin fluctuations $F(\boldsymbol{q}, \omega)$ which is the time Fourier transform of the calculated quantity $C(t)$. A non-exponential tail in $C(t)$ should appear at each $\boldsymbol{q}$ in $F(\boldsymbol{q}, \omega)$.

We have investigated these effects using the isotropic, short-range Heisenberg antiferromagnetic $KMn_{1-x}Ni_xF_3$. The transition temperature of the system varies with composition from 88–246 K as x goes from 0 to 1. The crystal structure is perovskite and thus the magnetic ions lie on a simple cubic lattice. The single crystal we used had $x = 0.7$ with $T_N = 210 \pm 2$ K and was previously investigated by Cowley and Carneiro [12]. It shows some smearing in its transition temperature which corresponds to a small amount of chemical inhomogeneity, which for our purposes is irrelevant as we did not intend to measure with precision any temperature dependences or critical exponents.

The experiments were performed using the triple-axis spectrometers IN12 and IN3 at the ILL, with pyrolytic graphite for both monochromators and analysers. On IN12 the experiments were performed with a fixed incident wavevector of 1.05 $Å^{-1}$ to give a resolution in energy of 8 GHz. The collimation was 60′, 60′, 60′ for the monochromator–sample, sample–analyser and analyser–detector respectively. A beryllium filter was used on the incident beam to remove the higher-order contamination. On IN3 a fixed final wavevector of 2.662 $Å^{-1}$ was used to give an energy resolution of 164 GHz and a graphite filter was used on the scattered beam to remove the higher-order contamination. For the IN3 measurements the collimation was 60′, 40′, 40′ for the monochromator–sample, sample–analyser and analyser–detector respectively. The sample was mounted in a variable-temperature cryostat with the $[0, 1, \bar{1}]$ direction vertical and scans in energy transfer were performed at various temperatures above T_N at a fixed wavevector transfer of (0.48, 0.48, 0.48) rlu close to the magnetic zone centre (0.5, 0.5, 0.5) rlu.

Comparison of the scans taken at the same temperature but at different resolutions allowed us to probe relaxation processes on different time scales. The IN3 data are

shown later in figure 1, and the higher-resolution IN12 data are shown later in figures 2 and 3. The full curves show the same model function fitted to both sets of data.

To analyse our data we define a counting rate (per monitor count) at the detector

$$J(\boldsymbol{q}_0, \omega_0) = I_0 \int_{\text{all } \boldsymbol{q}\text{-space}} \int_{-\infty}^{\infty} \mathrm{d}^3\boldsymbol{q}\, \mathrm{d}\omega\, S(\boldsymbol{q}, \omega) R(\boldsymbol{q} - \boldsymbol{q}_0, \omega - \omega_0) \tag{6}$$

where following [13] we define the resolution function for the three-axis spectrometer as a quadratic form

$$R(\boldsymbol{q} - \boldsymbol{q}_0, \omega - \omega_0) = R_0 \exp(-\tfrac{1}{2}\boldsymbol{x}\mathbf{M}\boldsymbol{x}) \tag{7}$$

where $\boldsymbol{x} = (\boldsymbol{q} - \boldsymbol{q}_0, \omega - \omega_0)$ and, $\mathbf{M} = \mathbf{M}(\boldsymbol{q}_0, \omega_0)$ is a symmetric matrix whose elements are given in [13] in terms of the instrumental parameters.

For a system of magnetic spins we make the usual factorisation into a static wave-vector-dependent susceptibility and a normalised spectral weight function or power spectrum

$$S(\boldsymbol{q}, \omega) = (n(\omega) + 1)\chi_{\boldsymbol{q}}^T F(\boldsymbol{q}, \omega) \tag{8}$$

where $F(\omega)$ is normalised so that

$$\int_{-\infty}^{\infty} \mathrm{d}\omega\, F(\boldsymbol{q}, \omega) = 1 \tag{9}$$

and $n(\omega)$ is the Bose population factor, which is slowly varying on the scale of the resolution and can be factorised out of the integral. Thus we have

$$J(\boldsymbol{q}_0, \omega_0) = I_0 \frac{V_F \sqrt{\det \mathbf{M}}}{4\pi^2} (n(\omega_0) + 1) \int \mathrm{d}^4\boldsymbol{x}\, F(\boldsymbol{q}, \omega) \chi_{\boldsymbol{q}}^T \exp(-\tfrac{1}{2}\boldsymbol{x}\mathbf{M}\boldsymbol{x}). \tag{10}$$

V_F is a factor given in equation (18) of [14] relating to the resolution volume of the secondary spectrometer. It is of importance for scans at constant incident wavelength and has the form

$$V_F \propto k_F^3 \cot \theta_A \tag{11}$$

where θ_A is the scattering angle at the analyser. It is the reason for the asymmetry of the scans in figure 2. The factor I_0 is a constant containing quantities such as the incident neutron flux and the effective volume of the sample and we treat it as being constant for scans taken on the same spectrometer under the same resolution conditions, but allow it to vary in order to normalise the data sets taken under different resolution conditions.

Under the conditions of this experiment, $\chi_{\boldsymbol{q}}^T$ varies slowly on the scale of the resolution function, so that the $\boldsymbol{q}$ integrals can be performed analytically to give

$$J(\boldsymbol{q}_0, \omega_0) = I_0 \frac{V_F \chi_{\boldsymbol{q}}^T}{\sqrt{(2\pi)}\sqrt{(M_{44}^{-1})}} (n(\omega_0) + 1) \int_{-\infty}^{\infty} \mathrm{d}\omega\, F(\boldsymbol{q}, \omega) \exp[-\tfrac{1}{2}(\omega - \omega_0)^2 / M_{44}^{-1}] \tag{12}$$

i.e. the four-dimensional resolution integral has been reduced to a one-dimensional convolution in energy. The value of the resolution width in energy $(M_{44}^{-1})^{1/2}$ was measured using a vanadium sample which is an incoherent elastic scatterer.

We rewrite equation (12) as an integral over time with the spectral weight function $F(\boldsymbol{q}, \omega)$ defined in the time domain

$$J(\boldsymbol{q}_0, \omega_0) = I_0 \frac{2V_F \chi_q^T}{\sqrt{(2\pi)}\sqrt{M_{44}^{-1}}} (n(\omega_0)+1) \int_0^\infty \mathrm{d}t\, C(t)R(t) \exp(-\mathrm{i}\omega t) \tag{13}$$

where

$$\begin{aligned} R(t) &= \int_{-\infty}^{\infty} \mathrm{d}\omega \exp(-\omega^2/2M_{44}^{-1}) \exp(-\mathrm{i}\omega t) \\ &= \sqrt{(2\pi)}\sqrt{(M_{44}^{-1})} \exp(-t^2 M_{44}^{-1}/2). \end{aligned} \tag{14}$$

We perform the Fourier transform, equation (13), using a model spin–spin correlation function $C(t)$ and a fast-Fourier transform, and we compare the calculated values of $J(\boldsymbol{q}_0, \omega_0)$ with our measured values. We then fit parameters defined within $C(t)$ using a maximum likelihood fitting routine, assuming the neutron counts to be distributed according to the Poisson probability distribution.

The theory predicts a stretched exponential form for the long-time limit of the spin–spin correlation function. For shorter times we do not expect it to have this form. For the intermediate time regime we assume a spin diffusive form. Thus we can define a staggered magnetisation density which follows the laws of hydrodynamics, the dynamics being determined by expansions of various currents and densities and by conservation laws. This approach gives $C(t) \sim \exp(-t/\tau)$, where τ is a phenomenological relaxation time. At very short times we assume that this breaks down and that the spins have a finite 'decorrelation time' which causes the correlation function to fall off much more slowly. We approximate this by assuming $C(t) = 1.0$ up to a cut-off time t_0 (the discontinuity in the gradient of $C(t)$ that this involves is effectively filtered out as a high-frequency transient in the Fourier transform procedure). The value of t_0 can be estimated as the inverse of the highest spin-wave or phonon frequency in the crystal depending on the details of the spin dynamics, i.e. whether they are dominated by spin-wave or phonon processes. We find a finite value of t_0 to be necessary to fit our data at high frequencies.

In detail we analysed our data with a sum of two relaxation functions

$$\begin{aligned} C(\boldsymbol{q}, t) &= \frac{\exp(-t/\tau) + A\exp[-(Bt)^\beta] + A_{\mathrm{cp}}}{\exp(-t_0/\tau) + A\exp[-(Bt_0)^\beta] + A_{\mathrm{cp}}} && t > t_0 \\ &= 1.0 && t < t_0. \end{aligned} \tag{15}$$

Note that $C(\boldsymbol{q}, 0) = 1.0$ ensures the normalisation of the spectral weight function. The first exponential decay is from spin diffusion and the second is the long-time tail. The constant A_{cp} is to describe any relaxation processes which are beyond our energy resolution, i.e. they form a magnetic contribution to a resolution-limited central peak. We find all three parts to be necessary to describe our data.

There are two main sources of background in an experiment like this. First there is a so-called room background which arises because of gamma rays and neutrons not coming through the spectrometer and because of noise in the electronics of the counting chain. This is very small (~2 counts per million on IN12) and is added to $J(\boldsymbol{q}, \omega)$. Secondly there is a background due to nuclear incoherent scattering from the sample. This is strictly elastic and it is assumed to be isotropic, any temperature and $\boldsymbol{q}$-dependence only coming from the Debye–Waller factor [15]. At our small wavevector transfers it is to a good approximation constant. It gives rise to a resolution-limited central peak in

Table 1. The parameters obtained from fitting the model function defined in equation (15) to the data as explained in the text. Parameters without errors were fixed in the fits. χ^2 is a measure of the goodness of the fit.

T (K)	χ_q	τ (10^{-12} s)	β	A_{cp}	B (THz)	A	χ^2
280	1.27	0.82	1.0	0.000(2)	0.018(2)	0.038(2)	3.92
			$0.87^{+0.30}_{-0.44}$	0.0	0.02(1)	0.04(2)	3.92
260	1.92	1.06	1.0	0.002(3)	0.008(1)	0.046(2)	4.15
			$0.50^{+0.11}_{-0.11}$	0.0	0.012(4)	0.07(1)	3.73
240	3.38	1.41	1.0	0.013(2)	0.016(2)	0.028(2)	2.80
			$0.23^{+0.11}_{-0.13}$	0.0	0.1(3)	0.11(9)	3.19
			0.667	0.012(2)	0.025(5)	0.040(2)	2.85
225	6.45	2.09	1.0	0.013(1)	0.031(5)	0.035(4)	2.56
			$0.30^{+0.11}_{-0.13}$	0.0	0.03(6)	0.07(4)	5.04
			0.5	0.013(1)	0.15(4)	0.11(3)	2.63
220	8.08	2.42	1.0	0.011(1)	0.039(9)	0.044(9)	1.90
			$0.34^{+0.14}_{-0.15}$	0.0	0.03(5)	0.06(3)	4.25
			0.5	0.011(1)	0.2(1)	0.15(6)	1.85

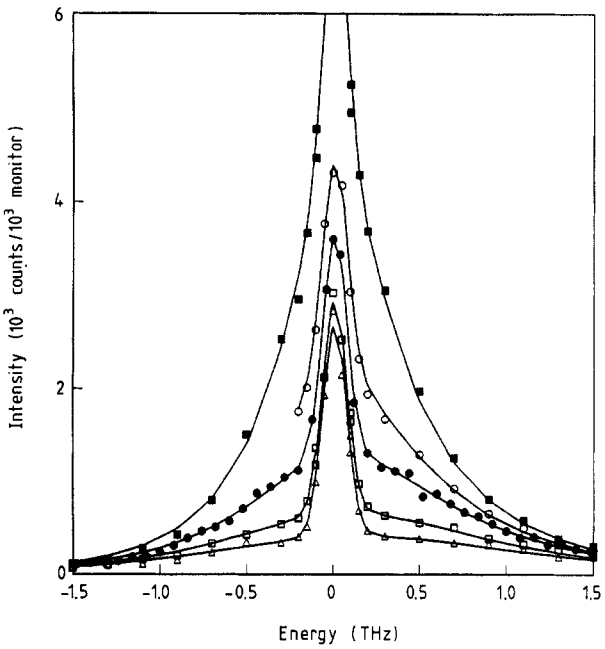

Figure 1. Data taken at various temperatures above T_N with a fixed final wavevector of 2.662 Å^{-1}. ■, 220 K; ○, 230 K, ●, 240 K; □, 260 K; △, 280 K. 10^3 monitor counts corresponds to approximately 3 minutes counting time. $\boldsymbol{q}$ = (0.48, 0.48, 0.48) rlu.

the measured power spectrum, the height of which should be independent of both $\boldsymbol{q}$ and temperature. In our analysis it is treated as a constant additive background to $C(\boldsymbol{q}, t)$, which was measured in scans well above T_N. The value of this enabled us to cross-normalise the two data sets and thus to use common fitted parameters in $C(t)$.

The value of t_0 was used as a fitting parameter in the widest of our low-resolution scans and found to be $0.65 \pm 0.1 \times 10^{-12}$ s. It was then left constant in the fits. For the low-resolution data the parameters τ, I_0 and A_{cp} were allowed to vary with $A = 0$, because any long-time tail is resolution limited in this case. Defining χ_q to be 1.0 at $T =$

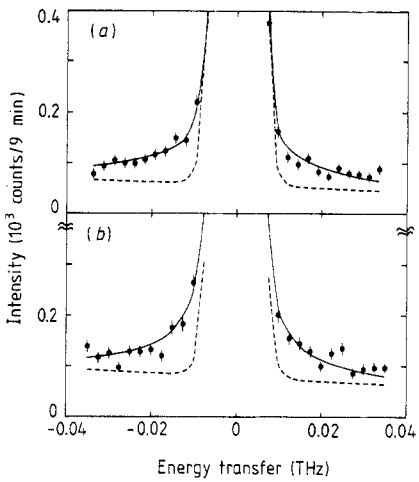

Figure 2. Data taken at various temperatures above T_G, with a fixed incident wavevector of 1.05 Å^{-1}: (*a*) $T = 280$ K, (*b*) $T = 260$ K. The full curves are the best fits to the model function including an exponential tail and the broken curves are calculated values assuming consistency with the data in figure 1, but with no long-time tail. $q = (0.48, 0.48, 0.48)$ rlu.

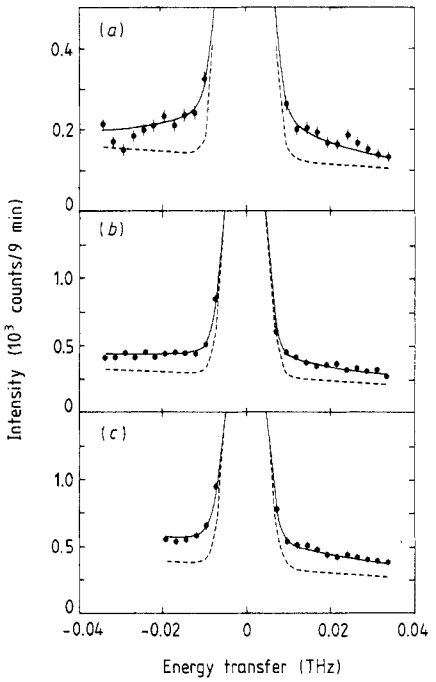

Figure 3. Data taken at various temperatures below T_G. (*a*) $T = 240$ K, (*b*) $T = 225$ K, (*c*) $T = 220$ K. Curve markings as in figure 2.

290 K we were thus able to find values for χ_q and τ at all the temperatures measured. The values obtained in this way were used in the fits to the high-resolution data to obtain values for the parameters β, B, A and A_{cp} (the values of either β or A_{cp} were fixed in the fits). The scans were cross-normalised by using different values for I_0, which were found to be 0.47×10^4 for the IN3 data and 0.35×10^7 for the IN12 data. Parameter sets obtained in this way are shown in table 1, together with a χ^2 merit function to show the relative quality of the fits at each temperature. The model function was then recalculated with these parameters for the low-resolution data to ensure consistency. The results of these calculations together with the data are shown in figure 1.

The data clearly show the existence of a long-time tail at all temperatures above T_N for which we have data. This can be seen for the scans above T_G in figure 2 and for the scans below T_G in figure 3. The broken curves in figures 2 and 3 show a calculated function without the presence of the second term in the model function, the spin diffusive term appearing as a flat background at this high resolution. At and below T_G there is also evidence for the existence of slower relaxation which was beyond the energy resolution of our experiment. However, we are able to assign it a relative weight with the parameter A_{cp}. In this way we can see a qualitative difference in the scans above and below T_G.

In the fits there are significant correlations between the values of β, B and A and so obtaining a unique set of values is not possible from our data. For this reason we show several sets of possible parameters in table 1. However, we are able to draw several qualitative conclusions from the fits. The data above T_G seem to be well described by a single exponential tail as in equation (4) with a time constant which is a decreasing function of $T - T_G$. We do not see evidence for the exponentially decreasing amplitude in equation (4). At and below T_G we see evidence for slow relaxation which we do not resolve, whose weight is roughly constant throughout the Griffiths phase. The tail that we do observe presumably forms part of a pre-asymptotic regime and is well described by a stretched exponential relaxation function. In the absence of any theoretical understanding of this regime it is difficult to draw any conclusions from the values of the fitted parameters, apart from the fact that approximately 10% of the spectral weight lies in this long-time tail thus introducing significant corrections to χ_q over a purely spin-diffusive picture.

In conclusion we have measured the power spectrum of the spin fluctuations above T_N in the Heisenberg antiferromagnet $KMn_{0.3}Ni_{0.7}F_3$, using two experimental resolutions to separate relaxation processes occurring on different timescales. We find evidence for the existence of a long-time tail above and below T_G, with relaxation which is much slower below T_G than above T_G.

We wish to thank L D Cussen for experimental assistance with some of the IN12 experiments, R A Cowley for the loan of the crystal and A J Bray for helpful comments on the manuscript. This work was stimulated by discussions with M A Moore, A J Bray and G J Rodgers.

References

[1] Dhar D 1983 *Stochastic Processes: Formalism and Applications* ed. S Agarwal and S Dattagupta (Berlin: Springer)
[2] Randeria M, Sethna J P and Palmer R G 1985 *Phys. Rev. Lett.* **54** 1321
[3] Bray A J 1987 *Phys. Rev. Lett.* **59** 586
[4] Bray A J 1988 *Phys. Rev. Lett.* **60** 720
[5] Griffiths R B 1969 *Phys. Rev. Lett.* **23** 17
[6] Jain S 1988 *J. Phys. C: Solid State Phys.* **21** L1045
[7] Ogielski A T 1985 *Phys. Rev.* B **32** 7384
[8] Lloyd R G, Mitchell P W, Ward R C C and Cherrill M 1988 *J. Physique Coll.* C8 1047
[9] Lifshitz I M 1964 *Adv. Phys.* **13** 483
[10] Haus J W and Kehr K W 1987 *Phys. Rep.* **150** 263
[11] Hohenberg P C and Halperin B I 1977 *Rev. Mod. Phys.* **49** 435
[12] Cowley R A and Carneiro K 1980 *J. Phys. C: Solid State Phys.* **13** 3281
[13] Cooper M J and Nathans R 1967 *Acta Crystallogr.* **23** 357
[14] Dorner B 1972 *Acta Crystallogr.* A **28** 319
[15] Marshall W and Lovesey S W 1971 *Theory of Thermal Neutron Scattering* (London: Oxford University Press) pp 76–80